

Direct electrocatalytic activity of chicken liver sulfite oxidase immobilized on binary self-assembled monolayer composed of separated domains having opposite charges

Pham Hong Phong

Institute of Chemistry, Vietnam Academy of Science and Technology

Received 11 August 2016; Accepted for publication 19 December 2016

Abstract

In this work, the final binary SAMs composed of 11-aminoundecanethiol (AUT) domains and 10-carboxy-1-decanethiol (MUA) domains on Au(111) substrate was used for immobilizing chicken liver sulfite oxidase (CSO) to study the direct electron transfer and detect sulfite anions. Scanning tunneling microscope images clearly showed the phase separation between AUT and MUA domains in the final binary SAMs prepared by the electrochemically selective replacement method. The electrochemical signals of CSO appeared on the voltammogram indicated that the direct electron transfer between the enzyme and the modified electrode could be obtained without electron mediator. The electrocatalytic currents of sulfite oxidation by CSO immobilized on the final binary SAMs were linearly dependent on their concentrations in solution with $R^2 = 0.988$, revealing a possibility in detection this anion by employing the bioelectrochemical sensor.

Keywords. Binary self-assembled monolayers, sulfite oxidase, oppositely charged domains.

1. INTRODUCTION

Biosensors based on the third generation, in which direct electron transfer is taken place between active sites deeply buried within enzyme and electrode, have superior selectivity because of operating in a potential window closer to the redox potential of the enzyme and therefore less prone to interfering reactions [1]. Among enzymes containing redox active sites, sulfite oxidase (SOx), an enzyme catalyzing the oxidation of sulfite to sulfate, contains the molybdenum complex cofactor (Moco) and a cytochrome b5-type (*cyt* b5) heme into different domains, which are connected by a flexible loop region. The catalytic activity of SOx strongly depends on the efficiency of the intramolecular electron transfer (IET) between the catalytic Moco domain and the *cyt* b5 domains. The IET process is assumed to be mediated by large domain motions of the *cyt* b5 domain within the enzyme. Further, conformational change is involved in the IET of SOx, in which electrostatic interaction may play the role in guiding the docking of the heme domain to the Moco domain prior to electron transfer. Thus, the interaction of SOx with charged surface may affect the mobility of the *cyt* b5 domain required for IET and consequently hinder SOx activation. Since, sulfite biosensing has been considerable to study the

direct ET to allow the fast, selective and accurate determination of sulfite without the need for significant sample preparation.

Though, the nature and details of the interactions between protein and electrode are far from clear. Since, a great number of efforts have been implemented to provide more knowledge on IET in SOx and its catalytic activity in oxidation process of sulfite. For example, studies of the structure of SO in its activated form [2], investigations of electron transfer within SO immobilized on different types of substrates [3-7], modification of the electrode surface for studying the adsorption and orientation of SO [8, 9], or study of the sensitive and selective detection of sulfite [10].

To contribute, in this work, the conformational change of chicken liver sulfite oxidase (CSO) on the Au(111) substrate was studied by employing the oppositely charged domains in the binary self-assembled monolayers(SAMs) composed of AUT and MUA having nanostructure. By using this binary SAM, the oppositely charged surface can be controlled by varying the domain density, which significantly affect the electrostatic interactions with CSO during immobilization, leading to the mobility of the *cyt* b5 domain required for IET and consequently hinder CSO activation. The catalytic activity of the adsorbed SO was examined by cyclic

voltammetry technique to obtain the catalytic oxidation of sulfite ions.

2. EXPERIMENTAL

2.1. Reagents

11-aminoundecanethiol hydrochloride (AUT), 10-carboxy-1-decanethiol (MUA) were purchased from Donjindo, and 2-hydroxyethanethiol (MeOH) was purchased from TIC Co. These chemicals were used as received. Chicken liver Sulfite oxidase (CSO) was purchased from Sigma without purification.

Water was purified through a Mili-Q system (Millipore Co.). All other chemical were of reagent grade and used without further purification. Au(111) substrates were prepared by vapor deposition of gold (99.99 % purity) onto freshly cleaved mica sheets (Nilaco, Japan) which was baked at 580 °C prior to the desorption and maintained at 580 °C during the deposition [11].

2.2. Preparation of the initial SAMs of AUT-MeOH

The initial phase-separated binary SAMs composed of AUT and MeOH were prepared by immersing Au(111) substrates for 24±5 h in ethanol solution of these thiols where the total concentration of thiols was kept at 1 mM. The composition of the initial SAMs was controlled by varying the molar ratio of MeOH, $\chi^{\text{sol}}_{\text{MeOH}}$, keeping C_{total} constant. Here, $\chi^{\text{sol}}_{\text{MeOH}}$ was defined by $\chi^{\text{sol}}_{\text{MeOH}} = C^{\text{s}}_{\text{MeOH}}/C^{\text{s}}_{\text{total}}$, and $C^{\text{s}}_{\text{total}} = (C^{\text{s}}_{\text{MeOH}} + C^{\text{s}}_{\text{AUT}})$, where C_i was molar concentration of i ($i = \text{MeOH}, \text{AUT}$). The initial SAMs was then rinsed with ethanol and dried in air.

2.3. Preparation of the final binary SAMs of AUT-MUA

After receiving the initial binary phase-separated binary SAMs, MeOH domains were then removed by applying a potential of -0.65 V for 20 minutes in a 0.5 M KOH. After MeOH removal, the substrates were rinsed with ethanol and dried in air. The substrates were then immersed in 1 mM solution of MUA for 15-20 min to form phase-separated binary SAMs of AUT-MUA.

2.4. Immobilization of CSO on the final binary SAMs of AUT-MUA

CSO was immobilized on the final binary SAMs

by immersing the SAM into the phosphate buffer solution, pH = 7.1, containing 50 μM CSO for 20 minutes. Excess CSO was washed off by the buffer solution.

2.5. Apparatus

Cyclic voltammetry for the reductive desorption of adsorbed thiols was used to examine a surface composition at each process of the replacement. The voltammograms were recorded in a desecrated 0.5 mol dm⁻³ KOH aqueous solution at scan rate of 20 mV/s at 25 °C. A Au(111) deposited mica coated with the SAM was mounted at the bottom of a cone-shape cell using an elastic O-ring. The surface area of the electrode was estimated to be 0.126 cm². The potential was referred to an Ag/AgCl (saturated KCl) electrode.

Cyclic voltammetry measurements of electrochemical signals of CSO and detection of sulfite were recorded in 10 mM phosphate buffer solution, pH = 7.1, at scan rate of 100 mV/s.

Scanning tunneling microscope (STM) images were taken with a NanoScope III (Digital Instruments). Pt80Ir20 tips were prepared by electrochemical etching and coated by Apiezon wax. In-situ STM measurements were carried out in 100 mM NaClO₄ solution in the constant-current mode.

3. RESULTS AND DISCUSSION

In order to prepare the Au(111) surface composed of oppositely charged domains of AUT and MUA, the selective replacement method has been used because coadsorption of AUT and MUA from a mixing solution of these alkanethiols forms a homogenous mixing state due to having similar alkyl chain length [11]. Thus, to attain the given purpose, the initial phase separated binary SAMs of AUT-MeOH was employed to remove MeOH domains by electrochemical technique as described in elsewhere [12]. Steps of preparation of the final phase separated binary SAMs of AUT-MUA from the initial SAMs have been investigated by cyclic voltammogram for reductive desorption of SAMs in KOH 0.5 M solution, as presented representatively at a value of $\chi^{\text{sol}}_{\text{MeOH}} = 0.3$ in Fig. 1a.

As seen, the voltammogram for reductive desorption of the initial binary SAMs of AUT-MeOH clearly shows two separated peaks at -0.65 V and -0.95 V, suggesting the formation of two separated domains composed of AUT and MeOH [11]. Since the value of charge (Q) estimated from the peak areas, the variation of Q by $\chi^{\text{sol}}_{\text{MeOH}}$ was described in Fig. 1b. The obtained results indicate

that the surface occupied by AUT molecules is inversely proportional with the $\chi_{\text{MeOH}}^{\text{sol}}$. Thus, the AUT domain areas on the electrode surface can be easily changed by $\chi_{\text{MeOH}}^{\text{sol}}$ in preparation of the initial binary SAMs. This is very meaningful in controlling the oppositely charged domains in the final binary SAMs of AUT-MUA as discussed later.

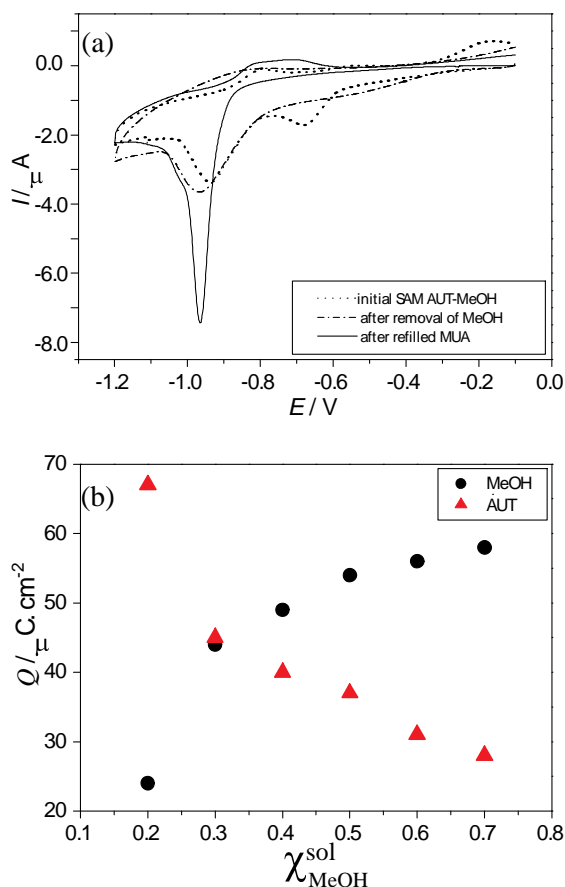


Figure 1: (a) CV for reductive desorption of the initial binary SAMs of AUT-MeOH at $\chi_{\text{MeOH}}^{\text{sol}} = 0.3$, after removal of MeOH domains, and the final binary SAM of AUT-MUA; (b) $\chi_{\text{MeOH}}^{\text{sol}}$ dependence on charges

It is different from the voltammogram recorded for the initial binary SAMs, the disappearance of the peak at -0.65 V on the voltammogram after removal of MeOH domains clearly indicates the complete removal of MeOH domains from the initial binary SAMs. After refilling MUA to vacant areas on the surface, the voltammogram shows only a sharp peak at -0.95 V. The appearance of a unique peak in this case can be explained by reduction of both AUT and MUA domains needed similar energy to desorb alkanethiol molecules from the Au(111) surface because of similar alkyl chain length in AUT and MUA molecules [11]. This interpretation is true because the phase separation in the final binary

SAMs of AUT-MUA can be clearly seen in STM images as shown in Fig 2. As seen, the number of bright spots decrease with increasing $\chi_{\text{MeOH}}^{\text{sol}}$, suggesting that bright spots are corresponding to AUT domain, meanwhile dark areas are attributed to MUA domains. This variation of domains is roughly correspondent to results obtained by the electrochemical method. Therefore, on the Au(111) substrate surface, the areas and density of oppositely charged domains can be controlled. This is because in previous study, it has been reported that domains of AUT and MUA possess positive and negative charges, respectively, on the surface due to the protonation and deprotonation of corresponding functional groups of $-\text{NH}_2$ and $-\text{COOH}$ [13].

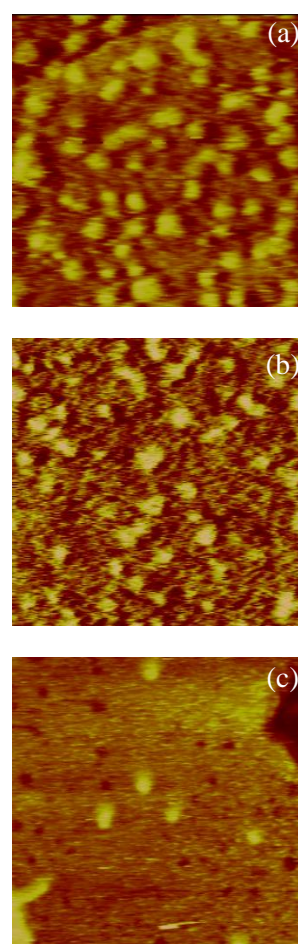


Figure 2: In-situ STM images recorded for the final binary SAMs of AUT-MUA prepared at various $\chi_{\text{MeOH}}^{\text{sol}}$: 0.3 (a); 0.5 (b); 0.7 (c). Images were recorded at set point = 300 pA

For the purpose of study, the final binary SAMs of AUT-MUA prepared from various values of $\chi_{\text{MeOH}}^{\text{sol}} = 0.0$ (single SAM of AUT), 0.3, 0.5, 0.7 were employed for investigating the immobilization of CSO by cyclic voltammetry. The obtained results indicated that the direct electron transfer (DET)

signal of CSO immobilized on the binary SAMs of AUT-MUA can only be appeared in the case of $\chi_{\text{MeOH}}^{\text{sol}} = 0.3$ as presented representatively in Fig. 3. This couple of weak peaks is attributed to the oxidation and reduction of the heme ($\text{Fe}^{2+}/\text{Fe}^{3+}$) [14]. The integration of peak gave a surface coverage of the enzyme, Γ , approximately 1.1 pmol.cm^{-2} of the electrochemically active site, assuming one e- transfer process.

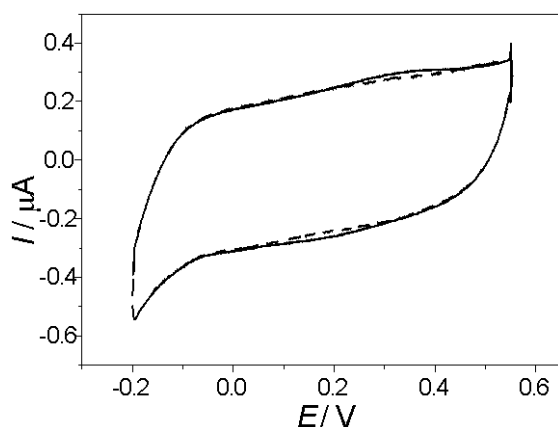


Figure 3: CV of CSO immobilized on the final binary SAMs of AUT-MUA domains prepared at $\chi_{\text{MeOH}}^{\text{sol}} = 0.3$ (solid line), and background curve (dotted line)

It is noticeable that CSO is an enzyme containing Moco and heme b5 cofactor domains linked by peptides singles. Each cofactor is preserved by amino acids strength forming charges. Use of theoretical approach combining steered molecular dynamics (SMD) and molecular dynamics (MD) all-atom simulation to obtain a 3D structural model of CSO gives a strongly negatively charged protein model with a net charge of $-36 e$ [15]. Therefore, during immobilization on the final AUT-MUA SAMs, the negative charge binding pocket preserved heme cofactor tends to binds AUT domains, meanwhile the positively charge binding pocket binds towards to MUA domains. This effect is able to result in changing a different position of *cyt* b5 domain, enabling a closer approach between both active sites. Thus, a conformation of SO molecules during adsorption on the surface due to the electrostatic interactions can be carried out at $\chi_{\text{MeOH}}^{\text{sol}} = 0.3$, at which there is an appropriate ratio of opposite charges on the electrode surface. This process makes the heme cofactor become well communicated to the modified electrode. This result indicates clearly the role of nano phase separated domains composed of oppositely charges in

orientation of SO molecules that supports the direct electron exchange between the heme domain within SOx and the modified electrode. This character is very useful for sensing sulfite ions by bioelectrochemical sensor using SOx immobilized on the final SAMs of AUT-MUA. It is similarly with the conformation of CSO in this work, the movement of *cyt* b5 has also been reported by other group [16].

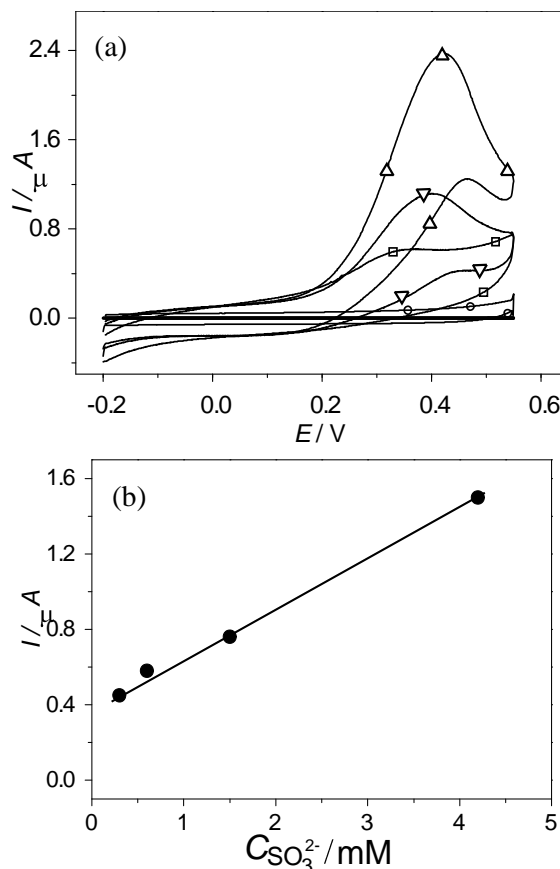


Figure 4: CV of sulfite oxidase immobilized on phase separated AUT-MUA SAM prepared at $\chi_{\text{MeOH}}^{\text{sol}} = 0.3$ recorded for various $C_{\text{SO}_3^{2-}} = 0.3$ (\circ); 0.6 (\square); 1.5 (∇); 4.2 mM (Δ), $v = 0.1 \text{ V/s}$ (a); and the calibration curve (b)

The catalytic activity of CSO immobilized on the final binary SAMs of AUT-MUA for oxidation of sulfite is depicted in Fig 4a. This figure shows cyclic voltammograms recorded for the catalytic activity of CSO immobilized on the final AUT-MUA SAMs at various concentrations of SO_3^- ($C_{\text{SO}_3^{2-}}$). An interesting effect quite different from the ideally catalytic current can be observed, that is the change in voltammogram shape with increasing $C_{\text{SO}_3^{2-}}$. At low concentrations, the expected sigmoidal shape was obtained and reached

the steady state, but the voltammogram became distinctly peak-shape as the $C_{\text{SO}_3^-}$ increased towards saturating levels. Particularly, a similar phenomenon has also been reported by other group when authors studied the direct catalytic electrochemistry of sulfite dehydrogenase [17] as well as modeled by other group as a convolution of two ideally sigmoidal voltammograms which are related by a redox switch at potential E_{sw} [18]. This evidence has been interpreted that the activity at high overpotential (driving force) was assumed to be lower than at moderate overpotentials, thus, leading to a maximum peak current that decreased to a plateau as the driving force increased. Since the obtained catalytic currents, their variation on $C_{\text{SO}_3^-}$ was found to be linear as shown in the calibration curve in Fig 4b. The relative equation is described as $y = 0.3869x + 0.2697$ with $R^2 = 0.998$.

4. CONCLUSION

The final phase-separated binary SAMs of AUT-MUA prepared by electrochemically selective replacement method used for studying the direct electron transfer of chicken liver sulfite oxidase to detect sulfite have been investigated. The obtained results reveal that electrostatic interactions between amino acids surrounded heme domains deeply buried within CSO and separated nano domains on the modified electrode surface play the role in the conformation of CSO to obtain the direct electron transfer. This behavior is very crucial for electrochemical catalyzing the direct oxidation of sulfite anions without electron mediator to form the third generation biosensor.

REFERENCES

1. Y. Wu, S. Hu. *Biosensor based on direct electron transfer in redox proteins*, *Microchim. Acta*, **159**, 1-17 (2007).
2. T. Utesch, M. A. Mroginski. *Three-dimensional structural model of chicken liver sulfite oxidase in its activated form*, *J. Phys. Chem. Lett.*, **1**, 2159-2164 (2010).
3. E. E. Ferapontova, Lo Gorton. *Direct electrochemistry of hememulticofactor-containing enzymes on alkanethiol-modified gold electrodes*, *Bioelectrochem.*, **66**, 55-63 (2005).
4. M. Senzr, R. Spricigo, T. Utesch, et al. *Redox properties and catalytic activity of surface-bound human sulfite oxidase studied by a combined surface enhanced resonance Raman spectroscopic and electrochemical approach*, *Phys. Chem. Chem. Phys.*, **12**, 7894-7903 (2010).
5. S. Frasca, O. Roias, J. Salewski, et al. *Human sulfite oxidase electrochemistry on gold nanoparticles modified electrode*, *Bioelectrochem.*, **87**, 33-41 (2012).
6. T. Zeng, S. Leimkuhlert, J. Koetz, U. Wollenberger. *Effective electrochemistry of human sulfite oxidase immobilized on quantum-dots-modified indium tin oxide electrode*, *Appl. Mater. Inter.*, **7**, 21487-21494 (2015).
7. T. Zeng, S. Frasca, J. Rumschottel, et al. *Role of conductive nanoparticles in the direct unmediated bioelectrocatalysis of immobilized sulfite oxidase*, *Electroanal.* DOI: 10.1002/elan.201600246 (2016).
8. E. E. Ferapontova, T. Ruzgas, Lo Gorton. *Direct electron transfer of heme-and molybdopterin cofactor-containing chicken liver sulfite oxidase on alkanethiol-modified gold electrodes*, *Anal. Chem.*, **75**, 4841-4850 (2003).
9. E. E. Ferapontova, A. Christenson, A. Hellmark, T. Ruzgas. *Spectroelectrochemical study of heme-and molybdopterin cofactor-containing chicken liver sulfite oxidase*, *Bioelectrochem.*, **63**, 49-53 (2004).
10. W. Sroysee, K. Ponlakheth, S. Chairam, et al. *A sensitive and selective on-line amperometric sulfite biosensor using sulfite oxidase immobilized on a magnetic-gold folatenanocomposite modified carbon paste electrode*, *Talanta*, **156**, 154-162 (2016).
11. Imabayashi S., Iida M., Hobara D., Feng Z. Q., Niki K., Kakiuchi. *Reductive desorption of carboxylic-acid-terminated alkanethiol monolayers from Au(111) surfaces*, *T. J. Electroanal. Chem.*, **428**, 33-38 (1997).
12. P. H. Phong. *Artificially phase separated ternary self-assembled monolayers composed of 11-aminoundecanethiol, 1-dodecanthiol and 10-carboxy-1-decanethiol on Au(111) prepared by electrochemically selective replacement technique*, *Vietnam J. Chem.*, **53**, 166-169 (2015).
13. P. H. Phong. *Oppositely charged state formation of the homogenous binary self assembled monolayers composed of 10-carboxy-1-decanethiol and 11-amino-1-undecanethiol on Au(111)*, *J. Adv. Nat. Sci.*, **9**, 191-196 (2008).
14. E. E. Ferapontova, A. Christenson, A. Hellmark, T. Ruzgas. *Spectroelectrochemical study of heme-and molybdopterin cofactor-containing chicken liver sulfite oxidase*, *Bioelectrochem.*, **63**, 49-53 (2004).
15. T. Utesch, MA. Mroginski. *Three-dimensional structural model of chicken liver sulfite oxidase in its activated form*, *J. Phys. Chem. Lett.*, **1**, 2159-2164 (2010).

16. C. Feng, R. V. Kedia, J. T. Hazzard, et al. *Effects of solution viscosity on intramolecular electron transfer in sulfite oxidase*, *Biochem.*, **41**, 5816-5821 (2002).
17. T. D. Rapson, U. Kappler, P. V. Bernhardt. *Direct catalytic electrochemistry of sulfite dehydrogenase: mechanistic insights and contrast with related Mo enzymes*, *Biochim. Et Biophys. Acta*, **1777**, 1319-1325 (2008).
18. S. J. Elliot, K. R. Hoke, K. Heffron, et al. *Voltammetric studies of the catalytic mechanism of the respiratory nitrate reductase from Escherichia coli: how nitrate reduction and inhibition depend on the oxidation state of the active site*, *Biochem.*, **43**, 799-807 (2004).

Corresponding author: **Pham Hong Phong**

Institute of Chemistry

Vietnam Academy of Science and Technology

No 18, Hoang Quoc Viet, Cau Giay, Hanoi

E-mail: phphong@ich.vast.vn; Telephone: (84)-4-38362008.